January 28, 1999

Simulation of the photomultiplier response

I. Fedorko, S. Tokár, ...

Dept. of Nuclear Physics, Commenius University, Mlynská dolina F1,
SK-84215 Bratislava, Slovakia

1 Introduction

Good undestanding of photomultiplier (PMT) response in the case when a few photoelectrons are created on photocathode (faint input light signals) is of a principlal value for finding out the global proporties of the PMT based spectrometric systems. So called single photoelectron analysis can be used for determinig of some important PMT characteristics, which can be used for finding out such calorimeter parameters like the energy conversion factor (GeV-to-photoelectrons) , etc. In this work we simulated the PMT responses in different regimes of the PMT with the metal chanel dynode system structure mainly for the purpose of single photoelectron analysis. The main goal was to optimize the PMT response function neeeded for the single photoelectron analysis of the metal channel PMTs like Hamamatsu R5900.

2 Simulation of photomultiplier response

The core of PMT response simulation consists in simulation of electron cascade multiplication process that occur in dynode system of PMT. This process essentially obeys Poisson law but, nonetheless, for correct understanding of the PMT response different physical phenomena (inhomogeneities, photoelectric effect on the first dynode, etc.) in the PMT should be taken into account. The correct PMT response function must reflects the PMT structure from the view point of light conversion and charge multiplication. The operating principles and construction of the PMT have in general four essential elements : a *photocathode*, an *electron-optical system*, an *electron multiplier* and an *anode*, which collects the electron flux. For our purpose the PMT processes can be devided in two independent parts :

- photoconversion and subsequent ph.e. collection,
- amplifications in dynode system an collection on the anode.

2.1 Photoconversion

We are supposed to have a pulsed source of light with the constant amplitude. A certain portion of the emmited photons are hitting the PMT photocathode

- this number is a Poisson random variable. The incident photons (picked up by photocathode) can produce ph.e.s via photoelectric effect. The conversion of photons into electrons and their subsequent collection is a random binary process. Therefore the distribution of the number of photoelectron collected from photocathode is a convolution of Poisson and binary proceses which again gives a Poisson distribution:

$$P_\mu(n) = \frac{\mu^n e^{-\mu}}{n!}, \tag{1}$$

where μ is the mean number of ph.e. emitted from the photocathode and $P_\mu(n)$ the propability that n ph.e.s will be obsered when their mean is μ. It is important to note that μ, defined as

$$\mu = m \cdot \eta \tag{2}$$

is characterising also the photocathode quantum efficiency η, where m is the mean number of photons hitting photocathode.

2.2 Charge multiplication

Dynode system multiplies input photoelectron signal via the effect of *secondary emission*. In our model the number of secondary electrons is assumed to obey Poisson law. Secondary emission coefficient is a function of incident electron energy. In electron multiplier, the energy of the electrons incident on each stage is a function of the potencial difference between the dynodes. So the emission coefficient n_i is

$$n_i = const \cdot (U_i)^\kappa \tag{3}$$

where U_i is voltage between $(i-1)^{th}$ and i^{th} dynode, κ is an exponent varying from 0.5 to 0.9, and *const* is inferred from gain.

$$G = \prod_{i=1}^{N} n_i \tag{4}$$

where N is the total number of stages. As can be seen from the above mentioned, the mean value of the secondary emission coefficient is a function of gain, repartion ratio and exponent κ

$$n_i = \left(\frac{G}{\left(\prod_{i=1}^{N} k_i\right)^\kappa} \right)^{\frac{1}{N}} \cdot (k_i)^\kappa \tag{5}$$

whee the repartion ratio $k_1 : k_2 : ...$ is the same like the ratio of the applied voltages $U_1 : U_2 : ....$ Using this equatiuon we can find secondary emission coefficient for each dynode.

2.3 Additional processes

In a realistic PMT there are some additional phenomena, which contributes to or influences the output signal. In the presented model there are taken into account for the PMT Hamamatsu R5900 four important sources of fluctuaction:

- photocathode inhomogeneity
- collection of the ph.e. on the 2^{nd} dynode,
- photoconversion of the incident photons on the 1^{st} dynode,
- inhomogeniety of the dynode system.

The 1^{st} source affects a various number of ph.e. emitted from photocathode. The emission coef. for ph.e. collected on the 2^{nd} dynode is

$$n_2 = const \cdot \left(U_1 + U_2 \right)^{\kappa} \tag{6}$$

while in this case the energy of ph.e. is function of the voltage difference between the photocathode and the 2^{nd} dynode. It's is to show that the ph.e.s created on 1^{st} dynode are amplified in dynodes system like the ph.e.s from photocathode, but the output charge is lower. A coefficient of secondary emission is depended not only on the energy of incident electron but also on the place of incidence. This inmogeniety of dynode chain is important mainly for 1^{st} dynode.

In some cases the output of dynode system, when the process is initiated by big number of photoelectrons ($n > 4$, can be aproximated by Gaussian distribution.

The agreement between aproximation and model response for a few photoelectron is investigated, with respect of gain 10^4 to 10^7. We suposed that model response is according to the aproximation for three an more photoelectron

2.4 Simulation precess

At the start of an event we are generated photons with $P_\mu(n)$. Each photon produces ph.e.s, where generated ph.e.s have Gauss distribution in the bounds of the standart deviations of efficiency η. This "real" ph.e.s enter into the dynode system witout loss. The electrons are multiplicated on dynodes singly. The secondary electrons obey Poisson law with mean value given by ( ). An outgoing electron produces new ones on the next dynode under the same law. If the number of electrons hitting dynode are bigger then a critical value (for presented results ~ 50), we stopped multiplication for each electron severally. The response of next dynode stage is generated by Gauss distribution with the mean value Q

$$Q = q \cdot n_i, \tag{7}$$

where q is the number of incident electrons and n_i is emission coefficient on the $i^{\rm th}$ dynode.

The additional processes are also taken into account in our model. The response of photoconversion on $1^{\rm st}$ dynode we can interpret like supplement chgarge, generated as well as normal case. For the electrons collected on the $2^{\rm nd}$ dynode is emission coef. given by ( ). The inhomogeniety of dynodes can be taken into account via Gauss fluctuation of the volue n_i.

3 Results

In our calculation we simulated an eight stage PMT with the gain from 10^4 to 10^7 assuming that the charge multiplication process is an ideal one, i.e. production of secondaries obeys Poisson law, no homogeneities are present,photoelectrons are created only on photocathode and collection efficiency is 100%.

The results of simulation are presented in Figs.1-4, where the ideal case charge distributions initiated by n $(= 0, 1, 2, 3, 4, and 6)$ photoelectrons are shown for gains 10^4, 10^5, 10^6, and 10^7. We can conclude from these figures that at gains $> 10^6$ the PMT response is symmetric (Gaussian) if the charge distribution is initiated by 3 or more photoelectrons. In all cases the response is asymmetric if $n \leq 2$. At low gains $(< 10^6)$ the asymmerty is noticeable also in the case of 3 photoelectrons.

On the Fig.5 is full deconvoluted spectrum of photomultiplier Hamamatsu R5900. The aplied voltage for measurement was 950V with voltage repartition 1.66:1.66:1...:1.66:2.17. The spectrum was deconvoluted by the function ...(see...).Results of deconvolution are sumarised in Table 3 and was used like input data for simulation. The comparison of the measured and ideal simulated spectrum is on the Fig.6. The mean value μ =2.3571 of the total number of ph.e. generated on photocathode was used for ideal case. One can see, the ideal case without other physical phenomena isn't successfull to describe the real response. On the Fig.7 is nonzero ($\sim$ 10) propability of collection of ph.e. on the $2^{\rm nd}$ dynode taken into account, it is one kind of option to explain source of the $1^{\rm st}$ peak in the real spectrum. From the Table 1 we can also take the exact number of ph.e. emitted from the photocathode and the $1^{\rm st}$ dynode. The comparison between the real spectra and model with the photoemission on the dynode is presented on Fig.8. It is well know, thet the secondary emission coefficient depends no only on the energy of incident electron, but also on the place of incidence. The simulation shows that it depends mainly for a few dynodes on the start of amplifier chain. Fig.9 we see that the model with accounting of phenomena of the photoemission on the $1^{\rm st}$ dynode and inhomogeniety of dynode system is according well to the real spectrum. Inhomogeniety for two first dynodes is 25%.

Name	Value	Error
μ	2.3571	0.1651
μ_{ph}	2.1220	0.0145
$\mu_{1^{st}}$	0.2351	0.0079
Q_0	8.7473	0.0409
σ_{Q_0}	2.4784	0.0447
Q_1	105.6640	0.6256
σ_{Q_1}	65.6709	0.5132
Gain	1648756.50	

Table 1: Parameters of LED spectra taken with Hamamatsu R5900 photomultilier at 950V.

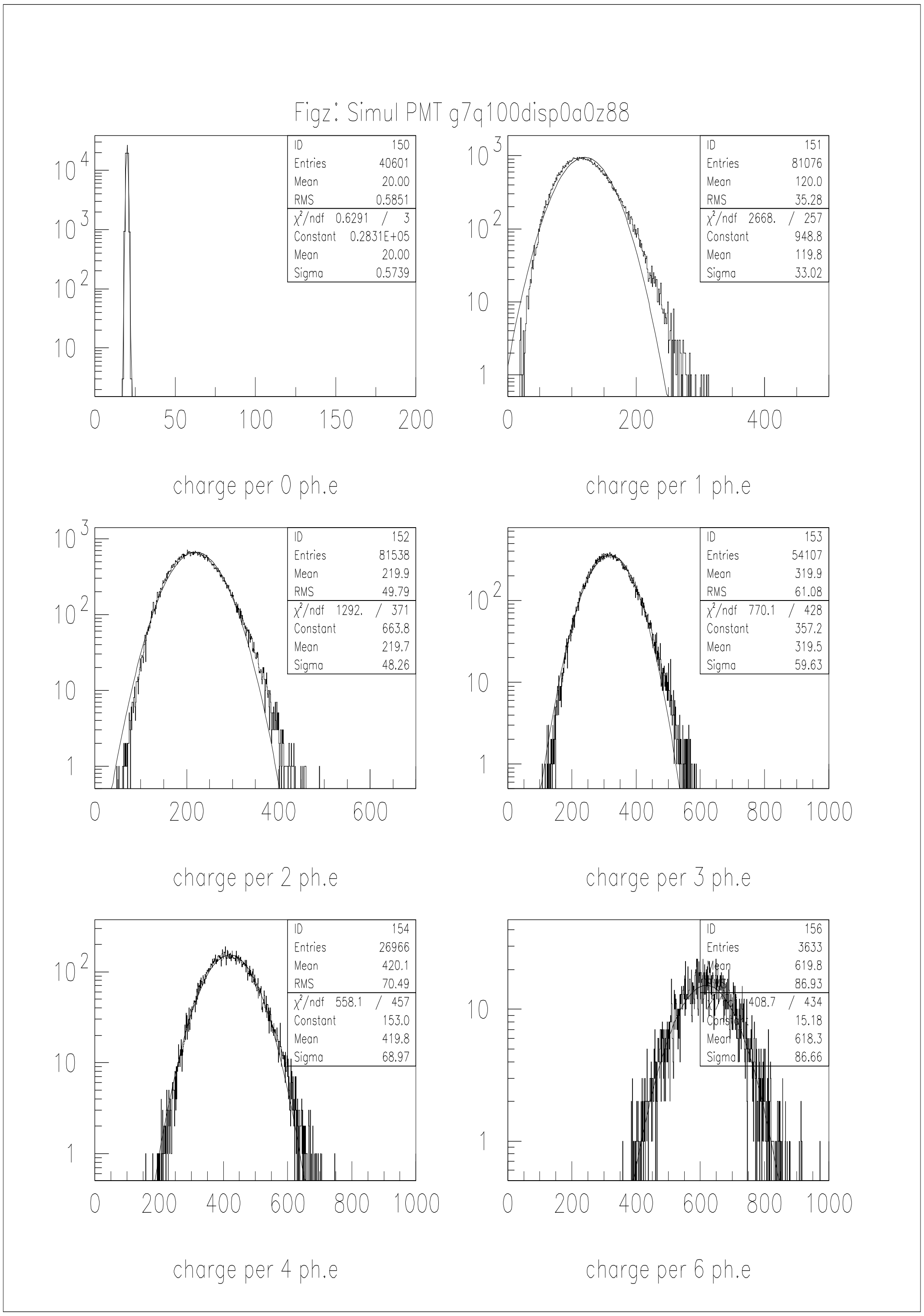

Figure 1: The output charge distributions initiated by different number of photoelectrons ($0-4$ and 6) at the PMT Gain 10^7.

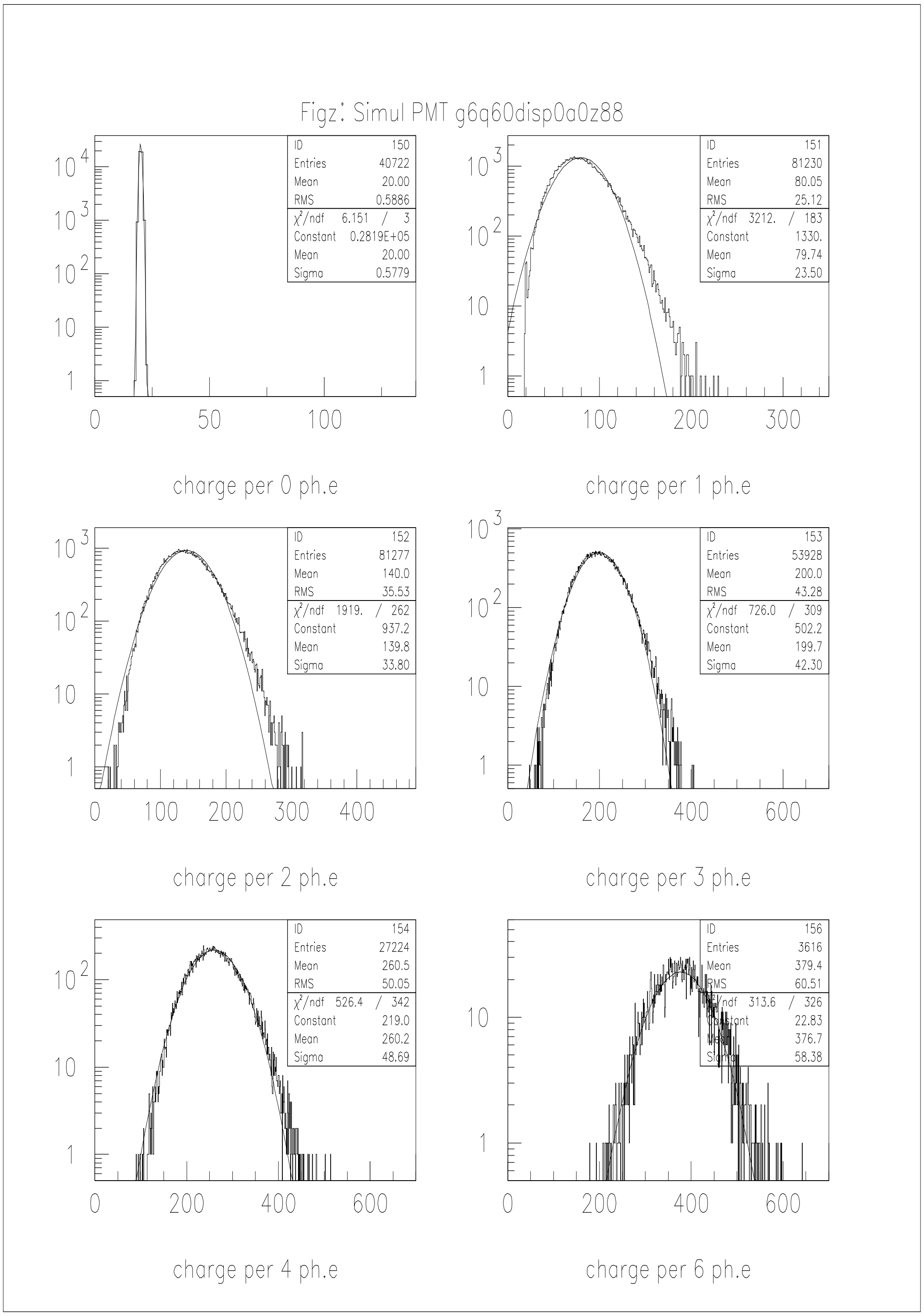

Figure 2: The output charge distributions initiated by different number of photoelectrons $(0-4$ and 6) at the PMT Gain 10^6.

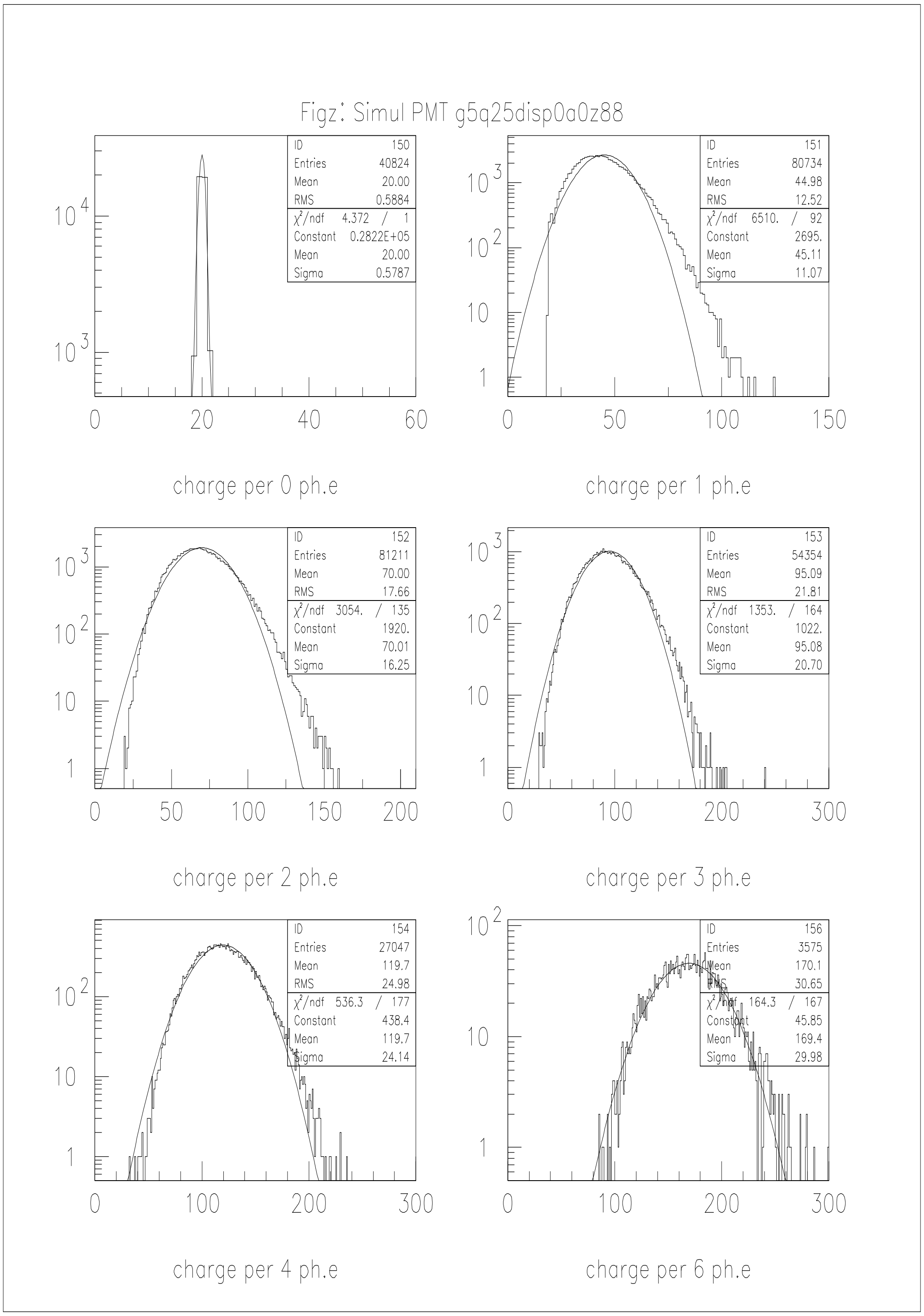

Figure 3: The output charge distributions initiated by different number of photoelectrons $(0-4$ and $6)$ at the PMT Gain 10^5.

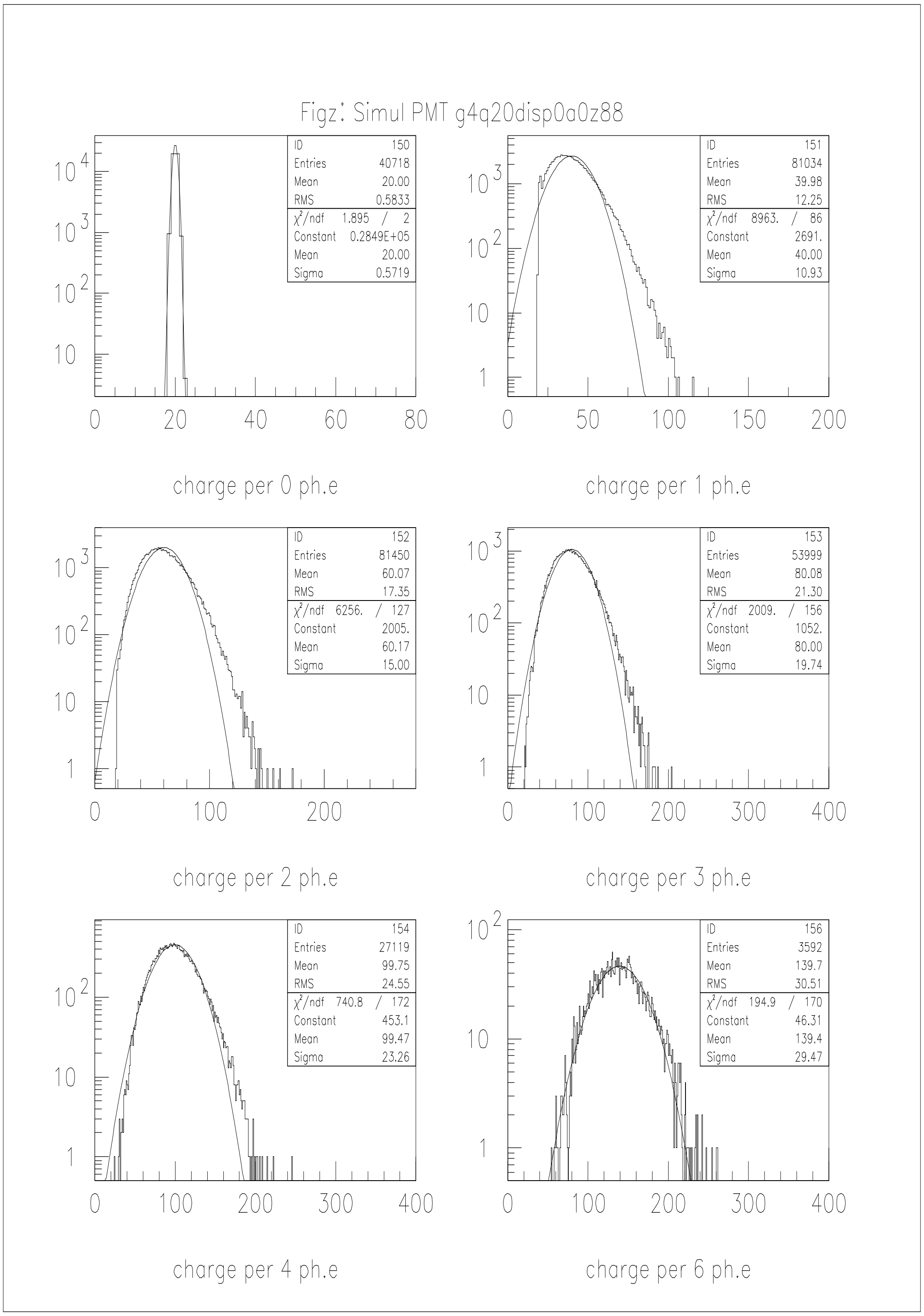

Figure 4: The output charge distributions initiated by different number of photoelect $(0-4$ and $6\ )$ at the PMT Gain 10^4.

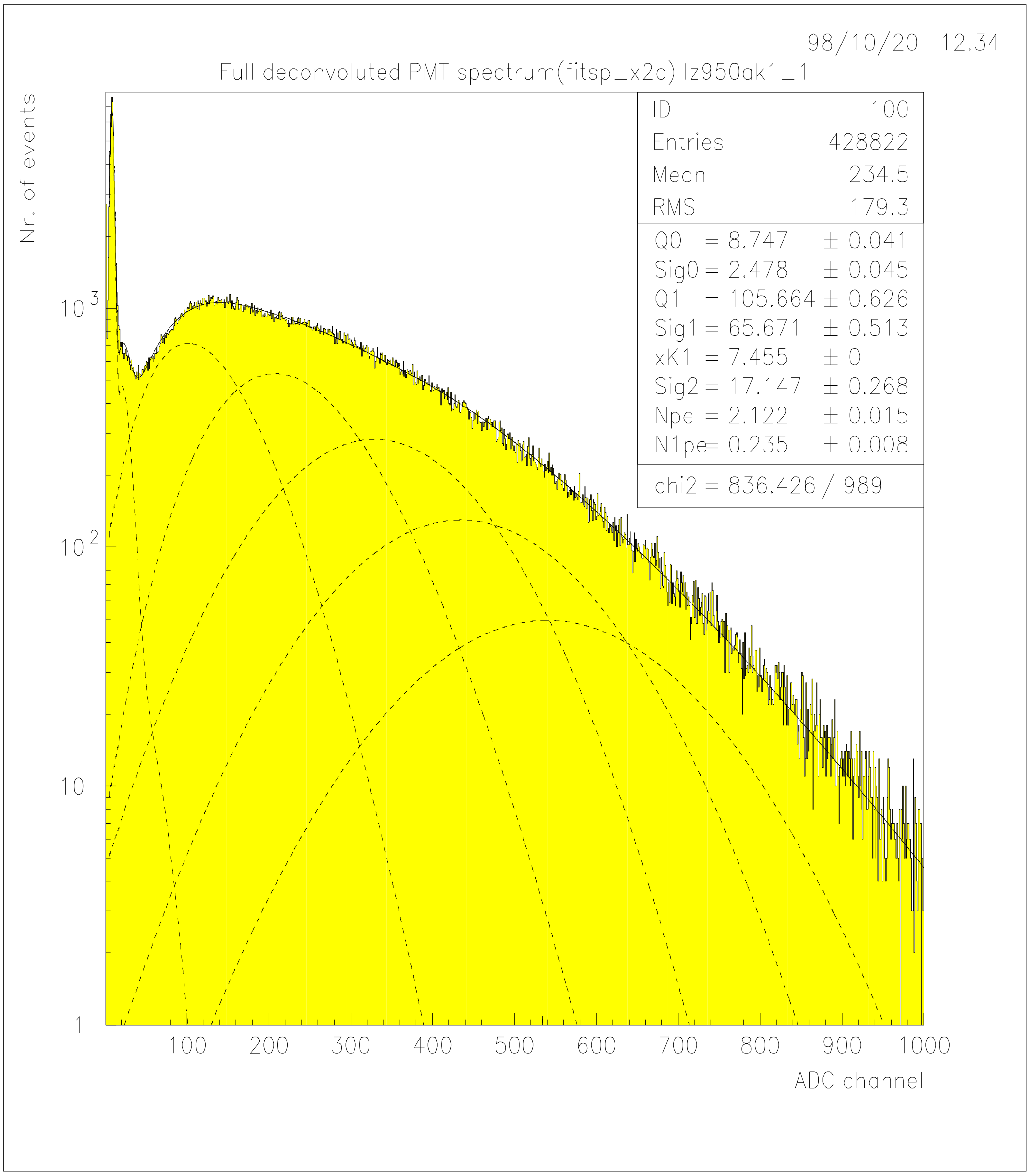

Figure 5: Typical deconvoluted LED spectrum (Hamamatsu R5900 photomultiplier).

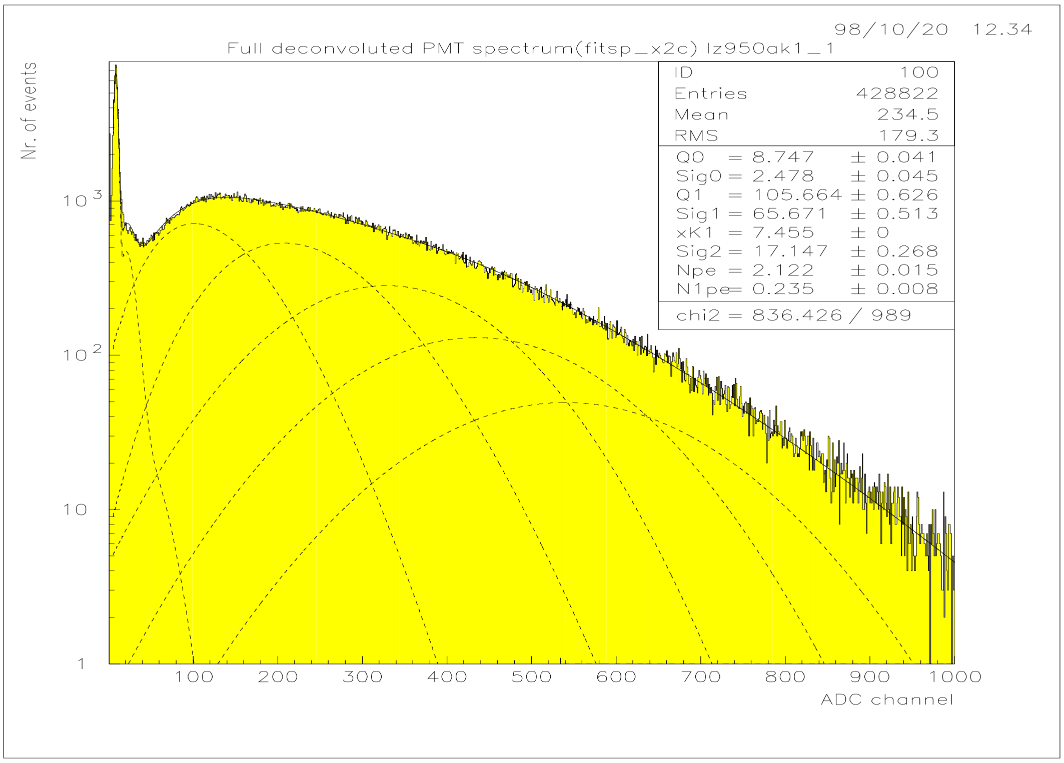

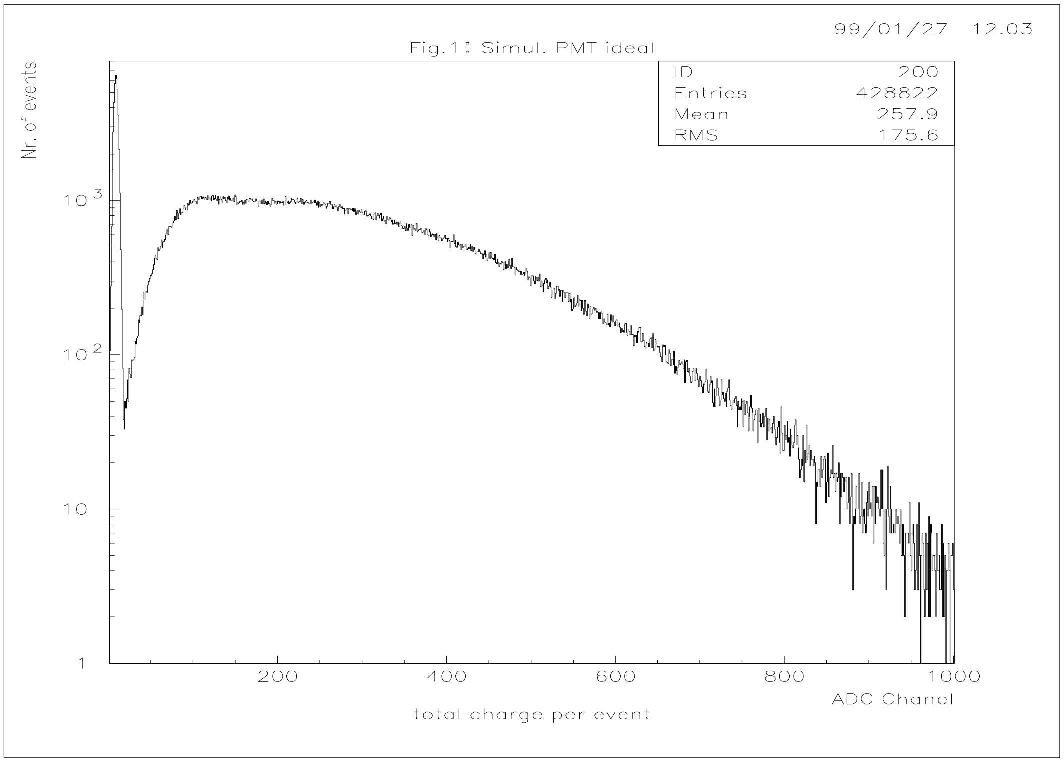

Figure 6: The total charge distributions : deconvoluted LED spectrum and simulated ideal response (at the PMT Gain $\sim 10^6$), respectively.

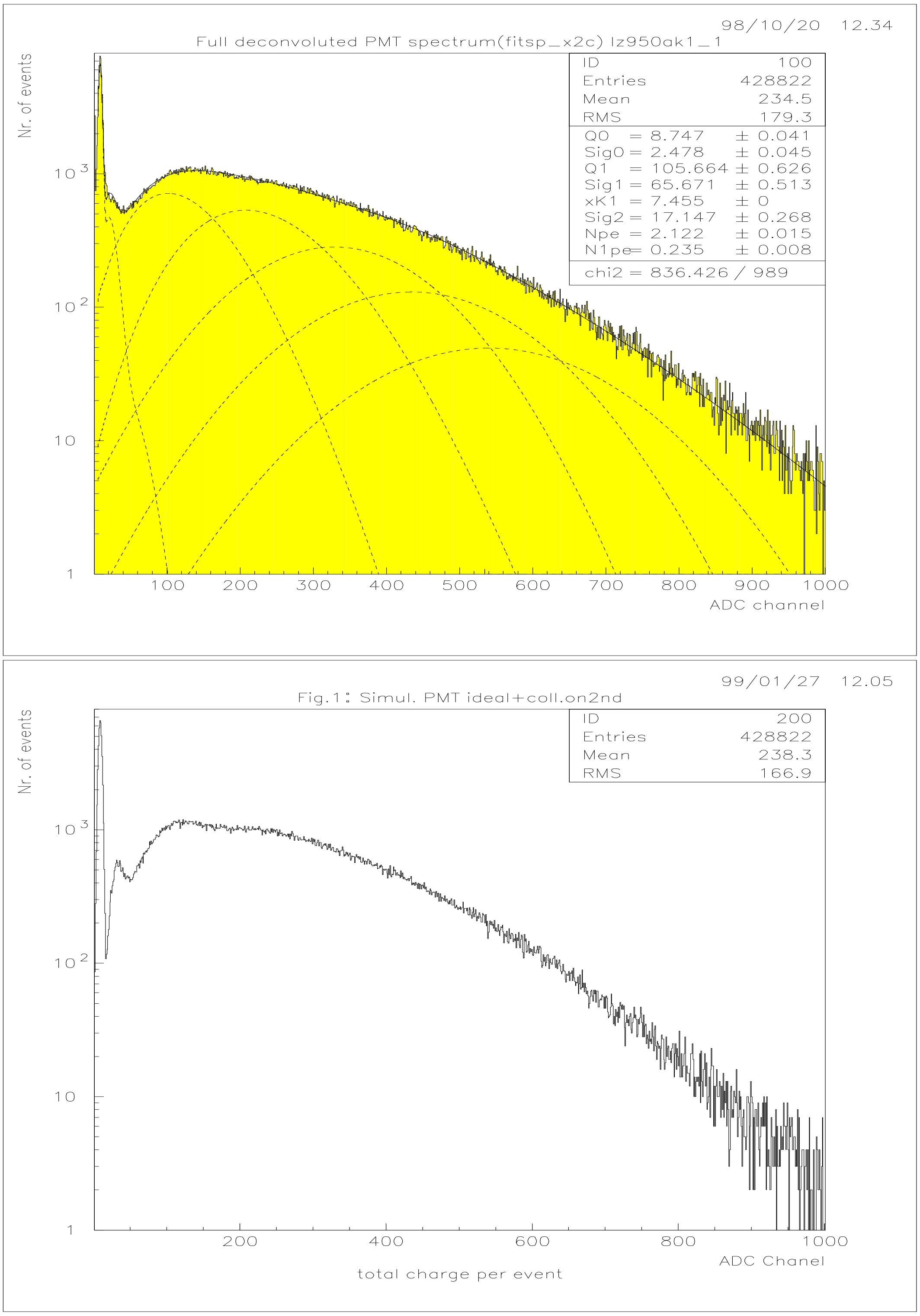

Figure 7: The total charge distributions : deconvoluted LED spectrum and simulated ideal response with the collection of ph.e. on the 2^{nd} dynode (at the PMT Gain $\sim 10^6$), respectively.

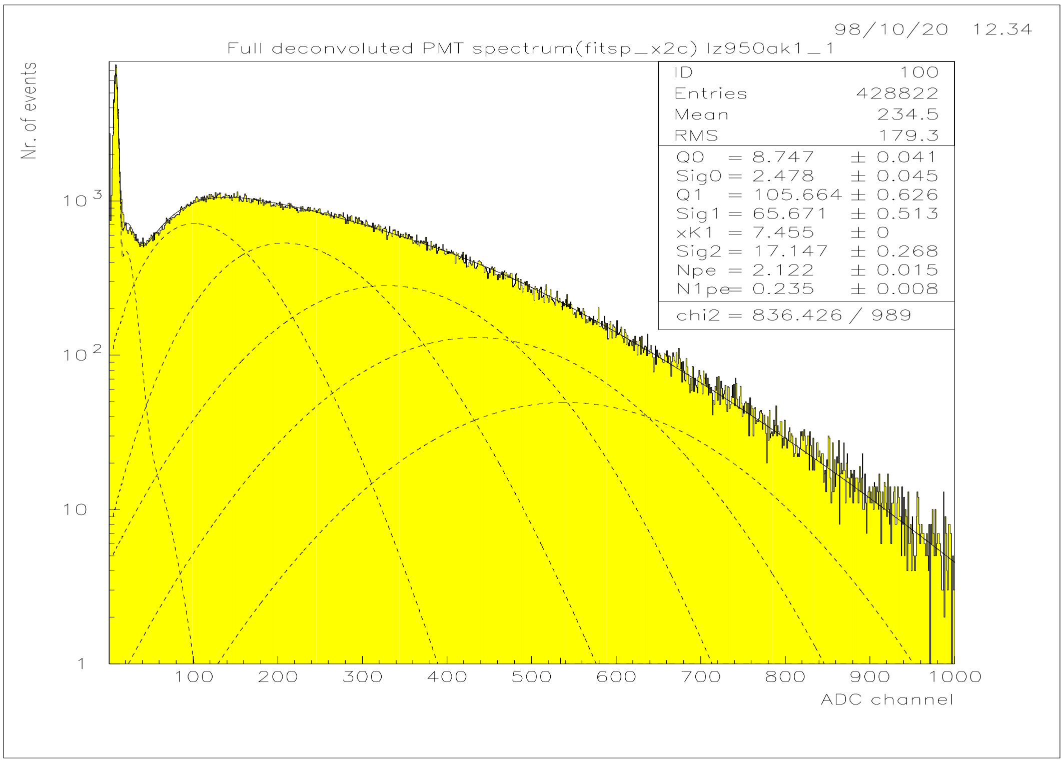

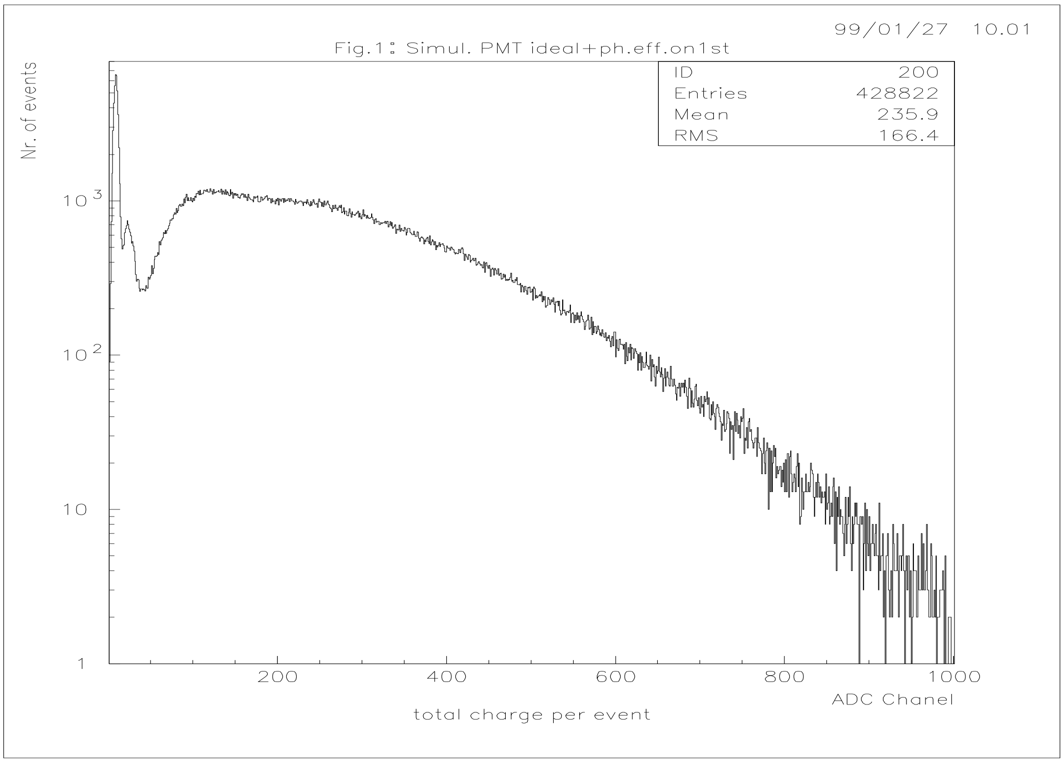

Figure 8: The total charge distributions : deconvoluted LED spectrum and simulated ideal response with the photoeffect on the 1^{st} dynode (at the PMT Gain $\sim 10^6$), respectively.

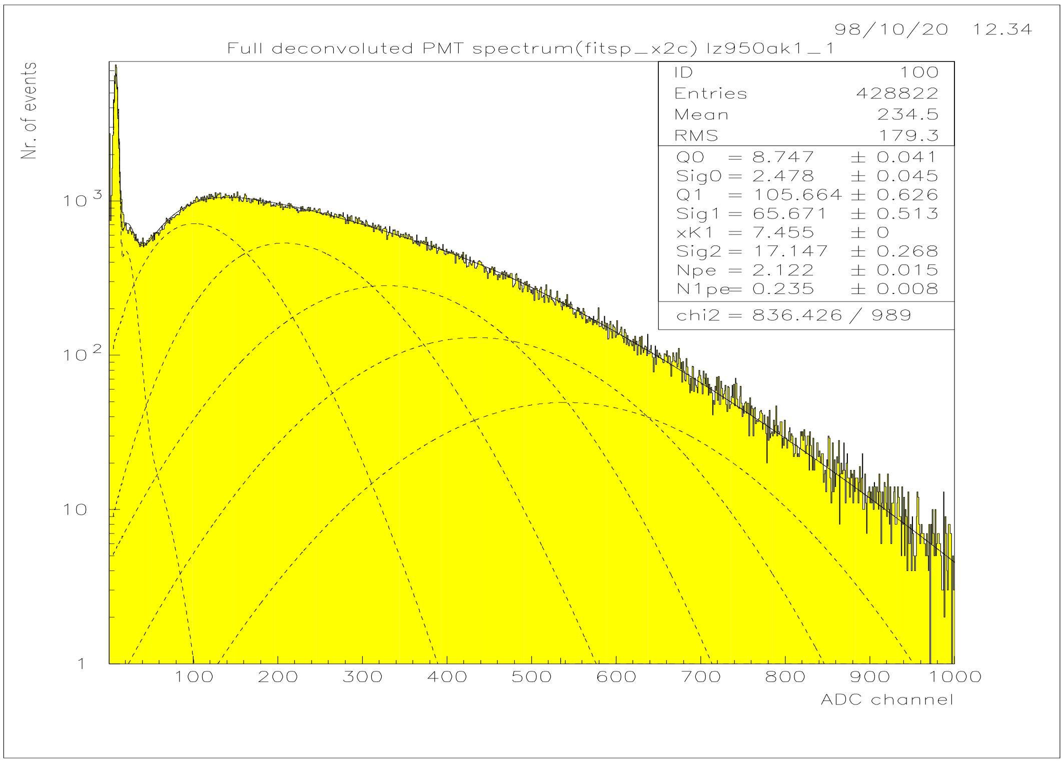

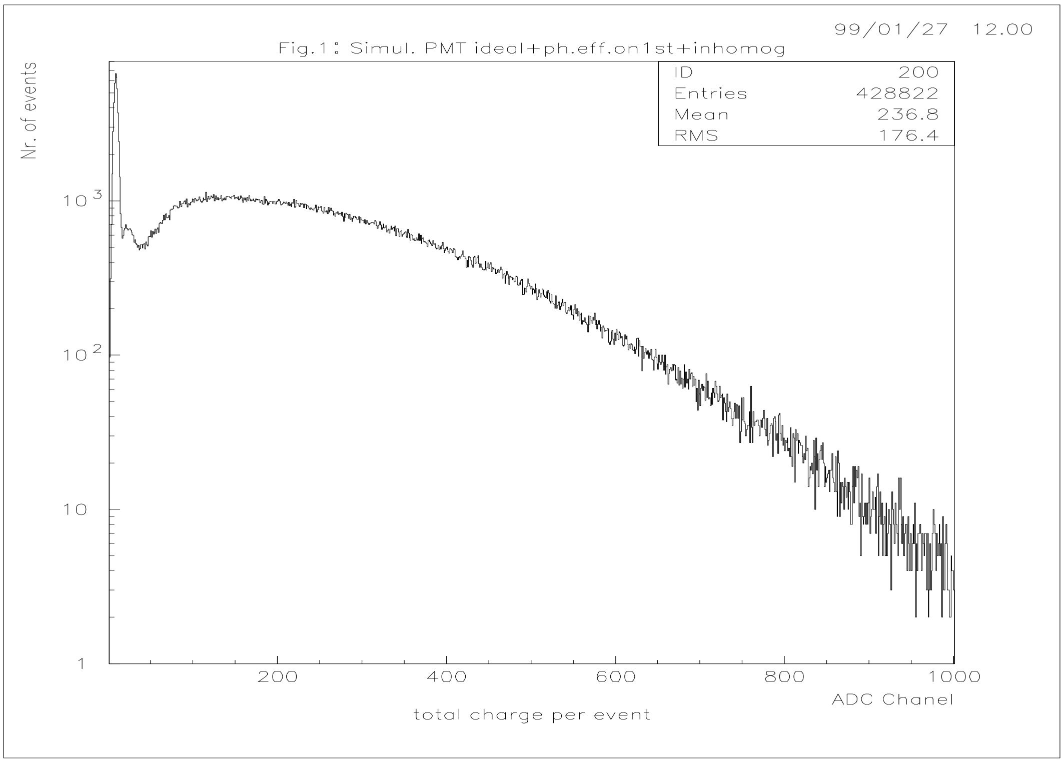

Figure 9: The total charge distributions : deconvoluted LED spectrum and simulated ideal response with the photoeffect on the 1^{st} dynode and inhomogeniety of emission coefficient (at the PMT Gain $\sim 10^6$), respectively.